Bioorganic & Medicinal Chemistry 21 (2013) 4831–4838

Contents lists available at SciVerse ScienceDirect

Bioorganic & Medicinal Chemistry

journal homepage: www.elsevier.com/locate/bmc

Novel imino sugar α-glucosidase inhibitors as antiviral compounds

J. D. Howe [a], N. Smith [a], M. J.-R. Lee [a], N. Ardes-Guisot [b], B. Vauzeilles [b,c], J. Désiré [d], A. Baron [c], Y. Blériot [d], M. Sollogoub [e], D. S. Alonzi [a], T. D. Butters [a,*]

[a] Oxford Glycobiology Institute, Department of Biochemistry, University of Oxford, South Parks Road, Oxford OX1 3QU, UK
[b] CNRS and Univ. Paris Sud, Glycochimie Moléculaire et Macromoléculaire, ICMMO, UMR 8182, Orsay F-91405, France
[c] Centre de Recherche de Gif, Istitut de Chimie des Substances Naturelles du CNRS, Avenue de la Terrasse, F-91198 Gif-sur-Yvette, France
[d] Institut de Chimie des Milieux et Matériaux de Poiteirs, UMR 7285, Equipe <Synthése Organique>, 4 rue Michel Brunet, Poitiers, F-8602, France
[e] UPMC Univ Paris 06, Institut Universitaire de France, Institut Parisien de Chimie Moléculaire, UMR-CNRS 7201, C. 181, 4 place Jussieu, 75005 Paris, France

ARTICLE INFO

Article history:
Available online 22 March 2013

Keywords:
Imino sugars
Neoglycoconjugates
Bovine viral diarrhea virus
Endoplasmic reticulum
Glucosidases

ABSTRACT

Deoxynojirimycin (DNJ) based imino sugars display antiviral activity in the tissue culture surrogate model of Hepatitis C (HCV), bovine viral diarrhoea virus (BVDV), mediated by inhibition of ER α-glucosidases. Here, the antiviral activities of neoglycoconjugates derived from deoxynojirimycin, and a novel compound derived from deoxygalactonojirimycin, by click chemistry with functionalised adamantanes are presented. Their antiviral potency, in terms of both viral infectivity and virion secretion, with respect to their effect on α-glucosidase inhibition, are reported. The distinct correlation between the ability of long alkyl chain derivatives to inhibit ER α-glucosidases and their anti-viral effect is demonstrated. Increasing alkyl linker length between DNJ and triazole groups increases α-glucosidase inhibition and reduces the production of viral progeny RNA and the maturation of the envelope polypeptide. Disruption to viral glycoprotein processing, with increased glucosylation on BVDV E2 species, is representative of α-glucosidase inhibition, whilst derivatives with longer alkyl linkers also show a further decrease in infectivity of secreted virions, an effect proposed to be distinct from α-glucosidase inhibition.

1. Introduction

Imino sugars are monosaccharide mimics in which the endocyclic oxygen has been replaced by nitrogen.[1] They have a number of advantages for compound design and synthesis to define biological activity. As polyhydroxylated molecules, each chiral centre offers manipulation to generate isomers with restricted or enhanced mimicry, and the endocyclic nitrogen atom is readily modified to gain selectivity, increase potency or improve pharmacodynamics. The properties of imino sugars have considerable potential for treating a diverse range of diseases, including lysosomal storage disorders,[2] cystic fibrosis,[3] and viral pathogenesis,[4,5] with a mechanism of action that is dictated by structural modification.[6] Two N-alkylated imino sugars, Miglitol and Miglustat, are approved medicines for the treatment of type II diabetes and Gaucher disease, respectively.[7]

Deoxynojirimycin is the imino sugar mimic of glucose, and its N-alkylated analogue *N*-butyl deoxynojirimycin (NB-DNJ) is an inhibitor of both the known DNJ based imino sugars' cellular targets ceramide glucosyl transferase (CGT), a key enzyme in the glycolipid biosynthetic pathway and the N-glycan processing enzymes of the ER, α-glucosidases I and II. NB-DNJ has been proposed as an effective treatment, known as 'substrate reduction therapy' (SRT), for a number of lysosomal storage diseases, in particular type I Gaucher disease for which clinical trials have been undertaken[8] and NB-DNJ (Miglustat, 'Zavesca') is an approved medicine in USA, Europe and Israel for this disorder.[9]

The class of DNJ neoglycoconjugates generated through click chemistry with functionalised adamantanes (Fig. 1) have previously been studied to gain structure activity relationship insights into their potential to inhibit both CGT and ER α-glucosidases I and II.[10] Following on from the initial insight into these cellular targets this paper attempts to consolidate our knowledge on this class of compounds by focussing on their potential to be antiviral, using the hepatitis C virus surrogate model, bovine viral diarrhea virus (BVDV). The mechanism of action behind the antiviral mechanism appears to be poorly understood but in the case of DNJ based imino sugars the inhibition of the ER glucosidases resulting in the disruption of the N-linked oligosaccharide processing pathway in the cell is a key factor.[11,12] However the ability of these compounds to inhibit CGT, any viral ion channels (such as P7 of HCV) plus any other unknown mechanism of actions provided by these intriguing molecules cannot be

* Corresponding author. Tel.: +44 (0) 1865 275725; fax: +44 (0) 1865 275216.
E-mail address: terry.butters@bioch.ox.ac.uk (T.D. Butters).

0968-0896/$ - see front matter © 2013 Elsevier Ltd. All rights reserved.
http://dx.doi.org/10.1016/j.bmc.2013.03.014

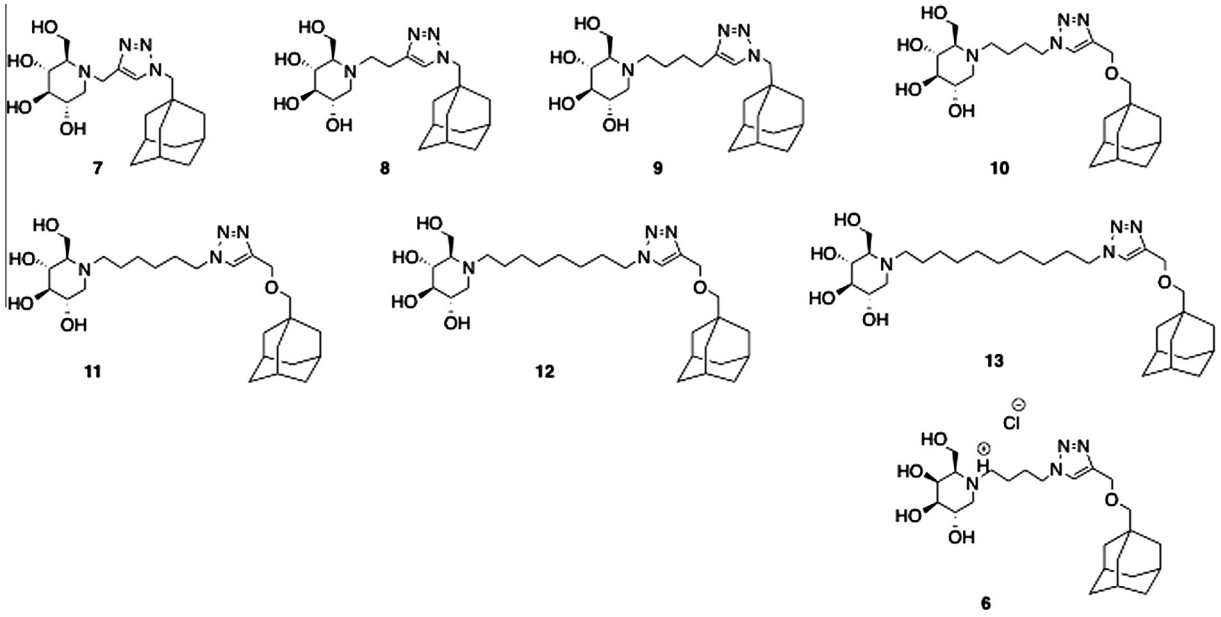

Figure 1. Structures of the adamantane–iminosugar conjugates. Structures of the adamantane–DNJ conjugates, previously synthesised and numbered.[10] The adamantane–DGJ conjugate **6**, the synthesis of which is described in this paper, is also shown for comparison.

discounted. Initially analysing the ER glucosidases inhibition by free oligosaccharide (FOS) analysis it is possible to differentiate in a cellular context the relative inhibitions of both α-glucosidases I and II and compare them to the antiviral capacity against BVDV to reveal the antiviral potential of these compounds.

2. Materials and methods

2.1. Materials

DNJ neoglycoconjugates were synthesized as previously described.[10] *N*-(4′-(4″-(Adamant-1-yl-methoxymethyl)-1*H*-1″-2″-3″-triazol-1″-yl)butyl)-1-deoxygalactonojirimycin hydrochloride **6** was synthesised from 2,3,4,6-tetra-*O*-benzyl-1-deoxygalactonojirimycin **1**, as shown in Scheme 1.

2.2. *N*-(4′-Azidobutyl)-2,3,4,6-tetra-*O*-benzyl-1-deoxygalactonojirimycin 3

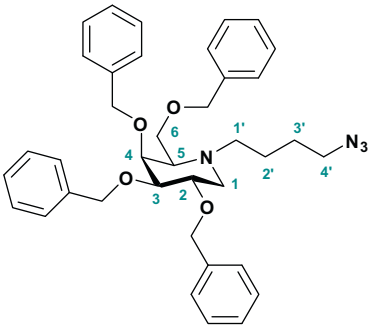

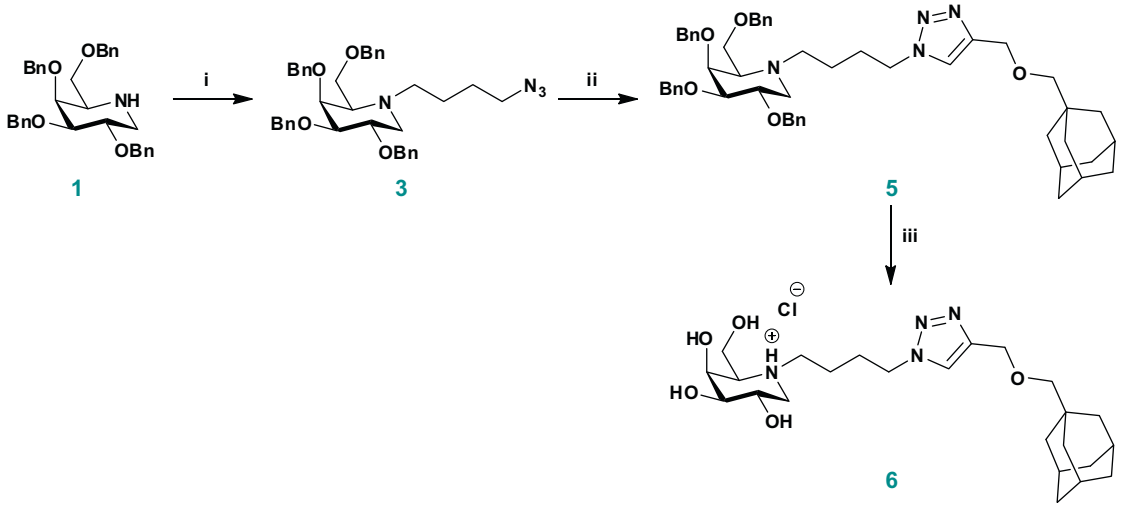

Scheme 1. Reagents and conditions: (i) (**2**), K_2CO_3, CH_3CN (65%); (ii) (**4**), $CuSO_4{\cdot}5H_2O$, sodium ascorbate, CH_2Cl_2/H_2O (1:1) (66%); (iii) HCl, Pd/C, H_2, EtOH (81%).

To a solution of 2,3,4,6-tetra-*O*-benzyl-1-deoxygalactonojirimycin (**1**) (114.6 mg, 0.22 mmol, 1.0 equiv) and 4-azidobutyl 4-methylbenzenesulfonate 2 (88.4 mg, 0.33 mmol, 1.5 equiv) in CH_3CN (3.0 mL) was added potassium carbonate (63.5 mg, 0.46 mmol, 2.1 equiv). The reaction mixture was refluxed at 85 °C for 24 h under an argon atmosphere then cooled. Most of the solvent was evaporated under reduced pressure. Water and CH_2Cl_2 were added to the residue and the whole mixture was stirred for 10 min, and then partitioned. The aqueous layer was extracted with CH_2Cl_2. The combined organic extracts were dried over sodium sulfate; filtrated and concentrated under reduced pressure. The residue was purified by flash chromatography over silica gel (Pet. ether/EtOAc 9:1 to 7:3) to yield 89.3 mg (0.14 mmol, 65%) of *N*-(4′-azidobutyl)-2,3,4,6-tetra-*O*-benzyl-1-deoxygalactonojirimycin **3** as a colorless oil.

2.3. *N*-(4′-Azidobutyl)-2,3,4,6-tetra-*O*-benzyl-1-deoxygalactonojirimycin 3

$C_{38}H_{44}N_6O_4$ R_f 0.33 (Pet. ether/EtOAc 8:2).

^{1}H NMR (500 MHz, CD_3CN) δ: 7.38–7.23 (m, 20H, 20 C*H* aromatic); 4.76 (d, 1H, ^3J 11.3 Hz, C*H*H Bn); 4.72 (d, 1H, ^3J 12.0 Hz, C*H*H Bn); 4.68 (d, 1H, ^3J 12.0 Hz, C*H*H Bn); 4.62 (d, 1H, ^3J 11.9 Hz, C*H*H Bn); 4.59 (d, 1H, ^3J 11.9 Hz, C*H*H Bn); 4.52 (d, 1H, ^3J 11.3 Hz, C*H*H Bn); 4.46 (s, 2H, CH_2 Bn); 4.00 (dd, 1H, $J_{4,5}$ 3.2, $J_{3,4}$ 2.6 Hz, H-4); 3.74 (ddd, 1H, $J_{1b,2}$ 7.9, $J_{2,3}$ 7.5, $J_{1a,2}$ 3.5 Hz, H-2); 3.72 (dd, 1H, $^2J_{6a,6b}$ 9.9, $J_{6a,5}$ 6.0 Hz, H-6a); 3.60 (dd, 1H, $^2J_{6a,6b}$ 9.9, $J_{6b,5}$ 4.9 Hz, H-6b); 3.53 (dd, 1H, $J_{2,3}$ 7.5, $J_{3,4}$ 2.6 Hz, H-3); 3.24 (t, 2H, J 6.4 Hz, 2 H-4′); 2.97 (dd, 1H, $^2J_{1a,1b}$ 12.2, $J_{1a,2}$ 3.5 Hz, H-1a); 2.88–2.76 (br s, 1H, H-5); 2.60 (dt, 1H, $^2J_{1'a,1'b}$ 13.0, $J_{1'a,2}$ 7.1 Hz, H-1′a); 2.52–2.40 (m, 1H, H-1′b); 2.26 (dd, 1H, $^2J_{1a,1b}$ 12.2, $J_{1b,2}$ 7.9 Hz, H-1b); 1.54–1.42 (m, 4H, 2 H-2′, 2 H-3′).

^{13}C NMR (125 MHz, CD_3CN) δ: 140.4–139.9 (4 Cq aromatic); 129.4–128.4 (20 CH aromatic); 77.2 (C-3); 76.3 (C-4, C-2); 74.5–72.7 (4 CH_2 Bn); 69.4 (C-6); 62.7 (C-5); 53.8 (C-1′); 52.2 (C-4′); 27.5, 24.1 (C-2′, C-3′).

MS (ESI$^+$): m/z 621.4 [M+H]$^+$. HRMS (ESI$^+$): calcd for $C_{38}H_{45}N_4O_4$ 621.3441, found 621.3470.

2.4. *N*-(4′-(4″-(Adamant-1-yl-methoxymethyl)-1*H*-1″-2″-3″-triazol-1″-yl)butyl)-2,3,4,6-tetra-*O*-benzyl-1-deoxygalactonojirimycin 5

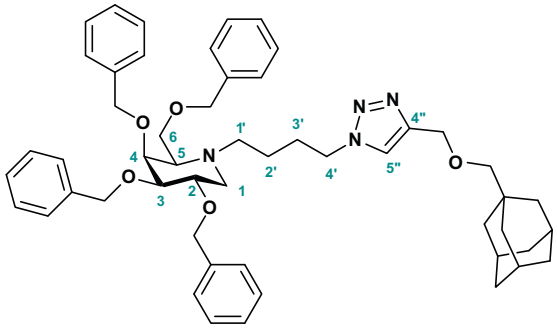

To a solution of *N*-(4′-azidobutyl)-2,3,4,6-tetra-*O*-benzyl-1-deoxygalactonojirimycin 3 (80.7 mg, 0.13 mmol, 1.0 equiv) and 1-((prop-2-yn-1-yloxy)methyl)adamantane **4** (39.8 mg, 0.19 mmol, 1.5 equiv) in CH_2Cl_2 (560 μL) and H_2O (423 μL) in a screw cap tube were added an aqueous solution of sodium ascorbate (97.5 μL, 0.2 M, 3.86 mg, 0.019 mmol, 15 mol %), followed by an aqueous solution of copper(II) sulfate (39.0 μL, 0.2 M, 1.95 mg, 0.008 mmol, 6 mol %). The reaction mixture was purged under argon, the cap screwed on and the solution then stirred at room temperature for 20 h. An aqueous saturated solution of sodium bicarbonate and $CHCl_3$ were added. The mixture was partitioned and the aqueous layer was extracted with $CHCl_3$, dried over sodium sulfate, filtrated and concentrated under reduced pressure. The residue was purified by flash chromatography over silica gel (Pet. ether/EtOAc 6:4) to yield 70.6 mg (0.086 mmol, 66%) of *N*-(4′-(4″-(adamant-1-yl-methoxymethyl)-1*H*-1″-2″-3″-triazol-1″-yl)butyl)-2,3,4,6-tetra-*O*-benzyl-1-deoxygalactonojirimycin **5** as a colorless oil.

2.5. *N*-(4′-(4″-(Adamant-1-yl-methoxymethyl)-1*H*-1″-2″-3″-triazol-1″-yl)butyl)-2,3,4,6-tetra-*O*-benzyl-1-deoxygalactonojirimycin 5

$C_{52}H_{64}N_4O_5$ R_f 0.23 (Pet. ether/EtOAc 6:4).

^{1}H NMR (500 MHz, CD_3CN) δ: 7.60 (s, 1H, H-5″); 7.38–7.24 (m, 20H, 20 C*H* aromatic); 4.75 (d, 1H, ^3J 11.3 Hz, CH*H* Bn); 4.71 (d, 1H, ^3J 12.0 Hz, CH*H* Bn); 4.67 (d, 1H, ^3J 12.0 Hz, CH*H* Bn); 4.61 (d, 1H, ^3J 11.9 Hz, CH*H* Bn); 4.58 (d, 1H, ^3J 11.9 Hz, CH*H* Bn); 4.52 (d, 1H, ^3J 11.3 Hz, CH*H* Bn); 4.46 (s, 2H, OCH_2Triazole); 4.44 (s, 2H, CH_2 Bn); 4.29 (t, 2H, J 7.1 Hz, 2 H-4′); 3.99 (dd, 1H, $J_{4,5}$ 3.2, $J_{3,4}$ 2.6 Hz, H-4); 3.76–3.72 (m, 1H, H-2); 3.72 (dd, 1H, $^2J_{6a,6b}$ 10.1, $J_{6a,5}$ 6.1 Hz, H-6a); 3.59 (dd, 1H, $^2J_{6a,6b}$ 10.1, $J_{6b,5}$ 4.7 Hz, H-6b); 3.55–3.50 (m, 1H, H-3); 3.03 (s, 2H, OCH_2Ad); 2.97–2.89 (br s, 1H, H-1a); 2.86–2.76 (br s, 1H, H-5); 2.61 (dt, 1H, $^2J_{1'a,1'b}$ 13.0, $J_{1'a,2}$ 7.4 Hz, H-1′a); 2.54–2.44 (br s, 1H, H-1′b); 2.28–2.20 (br s, 1H, H-1b); 1.93–1.88 (br s, 3H, 3 C*H*-Ad); 1.78 (tt, 2H, $J_{2',3'}$ 7.5, $J_{3',4'}$ 7.1 Hz, 2 H-3′); 1.74–1.59 (br m, 6H, 3 CH_2-Ad); 1.53–1.47 (br s, 6H, 3 CH_2-Ad); 1.39 (ddt, 2H, $J_{2',3'}$ 7.5, $J_{1'a,2'}$ 7.4, $J_{1'b,2'}$ 7.1 Hz, 2 H-2′).

^{13}C NMR (125 MHz, CD_3CN) δ: 146.0 (C-4″); 140.4–139.9 (4 Cq aromatic); 129.4–128.4 (20 CH aromatic); 123.9 (C-5″); 82.0 (OCH_2Ad); 77.2 (C-3); 76.3 (C-4, C-2); 74.3–72.7 (4 CH_2 Bn); 69.3 (C-6); 65.5 (OCH_2Triazole); 62.7 (C-5); 53.6 (C-1′); 50.7 (C-4′); 40.5 (3 CH_2-Ad); 38.0 (3 CH_2-Ad); 34.8 (Cq-Ad); 29.3 (3 CH-Ad); 29.0 (C-3′); 23.8 (C-2′).

MS (ESI$^+$): m/z 825.5 [M+H]$^+$. HRMS (ESI$^+$): calcd for $C_{52}H_{65}N_4O_5$ 825.4955, found 825.4970.

2.6. *N*-(4′-(4″-(Adamant-1-yl-methoxymethyl)-1*H*-1″-2″-3″-triazol-1″-yl)butyl)-1-deoxygalactonojirimycin hydrochloride 6

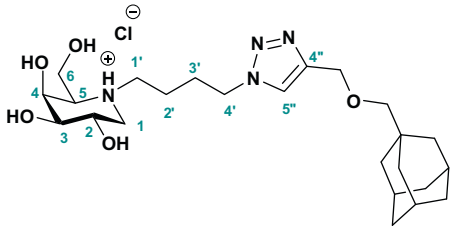

A solution of *N*-(4′-(4″-(adamant-1-yl-methoxymethyl)-1*H*-1″-2″-3″-triazol-1″-yl)butyl)-2,3,4,6-tetra-*O*-benzyl-1-deoxygalactonojirimycin **5** (64.0 mg, 77.6 μmol, 1.0 equiv) in ethanol (5.2 mL) was acidified to pH ~2 with 1 M aq HCl (10 drops). Argon was passed through the solution for 5 min, after which palladium 10%wt on carbon (58.8 mg, 0.54 mmol, 7.0 equiv) was added. Hydrogen was passed through the reaction mixture for 5 min and the reaction mixture was stirred for 5 days under atmospheric hydrogen pressure. Pd/C was removed by filtration over Celite® plug, followed by thorough rinsing with CH_3OH. The filtrate was

concentrated under reduced pressure. The residue was purified by flash chromatography over silica gel ($CHCl_3/CH_3OH$ 7:3) to yield 31.6 mg (63.1 μmol, 81%) of *N*-(4′-(4″-(adamant-1-yl-methoxymethyl)-1*H*-1″-2″-3″-triazol-1″-yl)butyl)-1-deoxygalactonojirimycin hydrochloride **6** as a white powder after freeze-drying.

2.7. *N*-(4′-(4″-(Adamant-1-yl-methoxymethyl)-1*H*-1″-2″-3″-triazol-1″-yl)butyl)-1-deoxygalactonojirimycin hydrochloride 6

$C_{24}H_{41}ClN_4O_5$ R_f 0.17 ($CHCl_3/CH_3OH$ 8:2).

^{1}H NMR (500 MHz, CD_3OD) δ: 7.96 (s, 1H, H-5″); 4.54 (s, 2H, OC*H*$_2$Triazole); 4.44 (t, 2H, *J* 7.1 Hz, 2 H-4′); 3.97 (dd, 1H, $J_{4,5}$ 3.2, $J_{3,4}$ 1.6 Hz, H-4); 3.84–3.78 (m, 2H, H-6a, H-6b); 3.80 (ddd, 1H, $J_{1b,2}$ 10.1, $J_{2,3}$ 9.2, $J_{1a,2}$ 5.0 Hz, H-2); 3.23 (dd, 1H, $J_{2,3}$ 9.2, $J_{3,4}$ 3.2 Hz, H-3); 3.06 (s, 2H, OC*H*$_2$Ad); 2.99 (dd, 1H, $^2J_{1a,1b}$ 11.2, $J_{1a,2}$ 5.0 Hz, H-1a); 2.82 (dt, 1H, $^2J_{1'a,1'b}$ 13.4, $J_{1'a,2'}$ 8.0 Hz, H-1′a); 2.56 (dt, 1H, $^2J_{1'a,1'b}$ 13.4, $J_{1'b,2'}$ 7.3 Hz, H-1′b); 2.44–2.38 (br s, 1H, H-5); 2.10 (dd, 1H, $^2J_{1a,1b}$ 11.2, $J_{1b,2}$ 10.1 Hz, H-1b); 1.96–1.88 (m, 3H, 3 C*H*-Ad); 1.89 (tt, 2H, $J_{2',3'}$ 7.7, $J_{3',4'}$ 7.1 Hz, 2 H-3′); 1.78–1.64 (br m, 6H, 3 C*H*$_2$-Ad); 1.57–1.52 (br m, 6H, 3 C*H*$_2$-Ad); 1.52 (ddt, 2H, $J_{1'a,2'}$ 8.0, $J_{2',3'}$ 7.7, $J_{1'b,2'}$ 7.3 Hz, 2 H-2′).

^{13}C NMR (125 MHz, CD_3OD) δ: 146.6 (C-4″); 125.0 (C-5″); 82.7 (OCH_2Ad); 77.2 (C-3); 72.7 (C-4); 69.0 (C-2); 65.6 (C-5, OCH_2Triazole); 62.7 (C-6); 57.8 (C-1); 53.3 (C-1′); 51.3 (C-4′); 40.9 (3 CH_2-Ad); 38.4 (3 CH$_2$-Ad); 35.2 (Cq-Ad); 29.9 (3 C*H*-Ad); 29.3 (C-3′); 22.7 (C-2′).

MS (ESI$^+$): *m*/*z* 464.3 [M−Cl]$^+$. HRMS (ESI$^+$): calcd for $C_{24}H_{41}N_4O_5$ 465.2077, found 465.3080.

2.8. Cell culture

Mardin-Darby Bovine Kidney (MDBK) cells (European Collection of Animal Cell Cultures, Porton Down, United Kingdom) were cultured in RPMI-1640 medium (PAA Laboratories, Teddington, UK) supplemented with 10% fetal calf serum (PAA), 2 mM L-glutamine (PAA) and 1× penicillin–streptomycin (PAA), at 37 °C in a humidified atmosphere containing 5% CO_2 (v/v).

2.9. Cell proliferation assays

A CellTiter 96R aqueous non-radioactive cell proliferation assay kit (Promega) was used to measure cellular cytotoxicity of compounds according to manufacturer protocol. MDBK cells were seeded in 96 well plates (5×10^3/well) and incubated for 24 h. Media was removed from wells and replaced with fresh media containing different concentrations of imino sugars shown in Figure 1, then incubated for a further 72 h.

40 μl of 3-(4,5-dimethylthiazol-2-yl)-5-(3-carboxymethoxyphenyl)-2-(4-sulfophenyl-2*H* tetrazolium) (MTS)–phenazine methosulfate mixture (20:1) were added to each well and the samples incubated for 1 h. The absorbance was read at 490 nm with a UVmax plate reader (Molecular Devices). Samples were analysed in triplicate and the concentrations at which absorbance at 490 nm was 50% of untreated controls (CC_{50}) were determined.

2.10. FOS analysis

MDBK cells were seeded in 6-well plates (1×10^6 cells/well) in medium containing different concentrations of imino sugars and incubated at 37 °C, 5% CO_2 atmosphere, for 24 h. After incubation, cells were harvested and free oligosaccharides (FOS) were extracted and purified as previously described.[13] FOS were labelled with 2-anthranilic acid,[14] and purified by chromatography using Discovery Speed Amide-2 columns.[13] The labelled FOS were further purified by chromatography using Concanavalin A (ConA)-Sepharose 4B columns (100 ml packed resin) as described previously (Alonzi et al., 2008), and then separated by NP-HPLC (Waters) using a 4.6 × 250 mm TSKgel Amide-80 column (Anachem),[14] as described previously.[15]

2.11. Fluorescence focus assay

MDBK cells were seeded in 6-well plates (1.75×10^6 cells/well) and infected with BVDV at an MOI of 1, followed by incubation with different concentrations of imino sugars for 24 h. Cell culture medium was then harvested and clarified by centrifugation at 5000 rpm for 10 min to remove cell debris. Serial dilutions were made and used to infect naive MDBK cells seeded in 96-well plates (7×10^4 cells/well). Cells were incubated for 24 h, then washed twice with cold PBS and fixed with 4% (v/v) paraformaldehyde in PBS for 30 min. Cells were washed again and blocked for two hours in 5% (w/v) milk in PBS. Cells were then permeabilised with 1% (v/v) Triton-X-100 in PBS for 20 min, washed with 1% (v/v) Tween20 in PBS and incubated with MAb103/105 (1:500 dilution in 5% milk-PBS; Animal Health Veterinary Laboratories Agency, Weybridge, UK) for 1 h. Cells were washed three times with 1% Tween20-PBS then incubated with anti-mouse FITC-conjugated secondary antibody (1:500 dilution in 5% milk-PBS; Sigma). Cells were washed again, and nuclei stained with 4′,6-diamidino-2-phenylindole (DAPI; Vector Laboratories Inc.). Cells were observed and evaluated using an inverted Nikon Eclipse TE200-U microscope, equipped with a Fluor 10× objective lens, and FITC and UV filter sets. Fluorescent foci were counted, and virus titers (fluorescent focus units (FFU)/ml) calculated.

2.12. Real-time RT-PCR analysis

MDBK cells were seeded in 6-well plates (1.75×10^6 cells/well) and infected with BVDV at an MOI of 1, followed by incubation with different concentrations of imino sugars for 24 h. Cell culture medium was then harvested and clarified by centrifugation at 5000 rpm for 10 min to remove cell debris.

A QIAamp viral RNA mini kit (Qiagen, Crawley, UK) was used to purify viral RNA from cell culture medium, according to manufacturer's protocol. The purified RNA samples were treated with DNase (20 min at 37 °C, followed by 10 min at 75 °C for deactivation). Real Time RT-PCR was carried out with a Qiagen SYBR green Quantitect RT-PCR kit, using primers that amplify a 334-bp portion of the NS2 coding sequence (forward primer, 5′-AGA AAA CAC AGA AAC CCG ACA GAC-3′; reverse primer 5′-TTC CAC CAC TAT TGT AGC ATC CG-3′). An Opticon 2 real time PCR machine (Bio-Rad) was used to perform the PCR reaction: 50 °C for 30, 15 min incubation at 95 °C followed by 35 cycles of 15 s at 95 °C, 1 min at 50 °C, 1 min at 72 °C and a final extension for 7 min at 72 °C. These data were calibrated against a standard curve produced using serial dilutions of a concentrated BVDV stock.

2.13. Immunoblotting

MDBK cells were seeded in 6-well plates (1.75×10^6 cells/well) and infected with BVDV at an MOI of 1, followed by incubation with different concentrations of imino sugars for 24 h. Cells were harvested by scraping in PBS and centrifuged at 2000 rpm for 5 min. The resulting pellet was briefly frozen at −20 °C then resuspended in PBS. The suspension was sonicated on ice using a Branson Sonifier (20 s, 50% duty cycle) to lyse cells. Protein concentrations were determined using a standard bicinchoninic acid protein assay. Proteins were then separated by sodium dodecyl sulfate–polyacrylamide gel electrophoresis (SDS–PAGE) under non-reducing conditions and transferred to Immobilon-P PVDF membrane (Millipore) by semi-dry electroblotting, then blocked overnight in 5% (w/v) milk, 0.2% (v/v) Tween20 in PBS. The

Table 1
Summary of cytotoxicity and α-glucosidase I and II maximal inhibition, as determined by FOS analysis

Compound alkyl linker C atoms	72 h Cytotoxicity CC_{50} (μM)	24 h FOS analysis in MDBK cells			
		Maximal α-glucosidase II inhibition (μM) and relative amount		Maximal α-glucosidase I inhibition (μM) and relative amount	
6 C4	>250	ni	ni	ni	ni
7 C1	>250	100	3.0	100	0.54
8 C2	>250	100	5.1	100	0.82
9 C4	>250	50	5.2	100	1.44
10 C4	>250	100	6.0	100	1.52
11 C6	205 ± 1.1	10	8.3	100	11.4
12 C8	51.7 ± 4.4	10	5.4	25	2.0
13 C10	29.2 ± 1.0	5	5.8	10	0.26

Cytotoxicity (CC_{50} values) is shown for each compound used in MDBK cells. FOS HPLC analysis was used to determine peak areas of mono- or tri-glucosylated $Man_5GlcNAc_1$ as indicators of inhibition of α-glucosidase II and I enzymes, respectively. Relative amounts in comparison to a control species $Man_4GlcNAc_1$ are shown. ni, not inhibitory.

membrane was incubated with MAb214 primary antibody (1:1000 dilution in blocking solution; Animal Health Veterinary Laboratories Agency) for 2 h at room temperature, washed extensively with PBS–0.1% (v/v) Tween20, then incubated with anti-mouse horseradish peroxidase secondary antibody (1:1000; Dako) for 1 h. Antibody binding to BVDV E2 protein was detected using Pierce ECL Western Blotting Substrate (Thermo Scientific, UK) and X-ray film (GE Healthcare, UK) by following the manufacturer's instructions.

3. Results

3.1. Cellular cytotoxicity increases with *N*-alkyl chain length

An MTS-based cell proliferation assay was carried out to determine the maximum concentrations of imino sugar derivatives that could be used without causing a significant effect to cell viability. The concentrations compounds **6**–**13** required to reduce proliferation in MDBK cells by 50% (CC_{50}) in 72 h are shown in Table 1. No significant cytotoxic effect was observed for compounds **6** **7**, **8**, **9** and **10**. More hydrophobic compounds showed greater anti-proliferative effects; **11** was 205 ± 1.1 μM, **12** was 51.7 ± 4.4 μM and **13** was 29.2 ± 1.0 μM. As the length of the alkyl linker between the imino sugar and the triazole ring increased, the CC_{50} decreased markedly, a property that has been noted for other N-alkylated iminosugars.[16]

3.2. ER α-glucosidase inhibition correlates with *N*-alkyl chain length

Previously, we showed that adamantyl–DNJ conjugates could inhibit cellular ER-glucosidases.[10] Free oligosaccharide (FOS) analysis of MDBK cells following inhibitor treatment was used to determine the level of in cellulo inhibition of ER α-glucosidases I and II. Inhibition of α-glucosidase II is known to cause an accumulation of monoglucosylated FOS, whilst inhibition of α-glucosidase I results in triglucosylated FOS accumulation. FOS species were purified from cells and separated by NP-HPLC for analysis. $Man_4GlcNAc_1$, which remained in constant amount over all concentrations of inhibitor used in this study, was used as standard and the relative amounts of mono- and tri-glucosylated $Man_5GlcNAc_1$ species were measured as representative markers of α-glucosidase II and I inhibition respectively (Fig. 2). Concentrations for maximal α-glucosidase I and II inhibition for each compound is shown in Table 1. Maximal α-glucosidase II inhibition was achieved for all compounds tested below the maximum concentration used. α-Glucosidase I inhibition occurred at higher concentrations and little inhibition was observed for compounds with short alkyl linkers. Treatment with 100 μM **11** showed the highest level of α-glucosidase I inhibition (Fig. 2B), more than three times higher than any other compound tested (Table 1). Compounds **9** and **10**) have alkyl linkers of the same length, differing only in the introduction of an ether bond between the triazole and the adamantyl group in **10**. The two compounds exhibited very similar ER α-glucosidase inhibition. Adamantyl–DGJ had no effect on α-glucosidase activity, in agreement with our previously published data using N-alkylated-DGJ compounds.[6]

3.3. Antiviral activity correlates with ER α-glucosidase inhibition

Compounds were screened for their ability to inhibit the biogenesis and infectivity of bovine viral diarrhea virus (BVDV). Viral production and release from MDBK cells was determined using RT-PCR to measure viral RNA copies secreted (Fig. 3A). Compounds were initially administered at 10 μM and at this concentration, short alkyl chain compounds **7**, **8** and **9** showed no antiviral activity, although **8** and **9** were effective when a higher concentration was used (50 μM, Fig. 3A). Reduction in RNA copies increased as alkyl chain length increased, with 10 μM **13** treatment reducing viral RNA fourfold. At 10 μM, **10** reduced RNA copies approximately twofold whereas **9** showed no effect, suggesting that the introduction of the ether bond between the triazole and the adamantyl group increases antiviral activity.

Infectivity of viral particles secreted from MDBK cells was determined as focus-forming units/ml (FFU/ml), by inoculating naive MDBK cells with virus secreted from cells administered with compound, then probing for BVDV NS2/3 protein (Fig. 3B). Compounds were tested at the same concentrations as for RT-PCR analysis, and reduction in FFU/ml mirrors the reduction in viral RNA copies for compounds **7** through **13**. Adamantyl-DGJ at 10 μM however showed no significant reduction in viral RNA and a small reduction in FFU/ml compared to the untreated control. Increasing the concentration of this compound to 50 μM revealed similar data (results not shown) indicating that inhibition of ER-α-glucosidases appeared essential to the antiviral activity of the DNJ neoglycoconjugates.

3.4. ER α-glucosidase inhibition increases glucosylation of intracellular BVDV E2 protein

Inhibition of ER α-glucosidases I and II by N-alkylated DNJ prevents deglucosylation of BVDV E2 protein (Lee et al., manuscript in preparation). MDBK cells were infected with BVDV (MOI = 1), then administered with compounds **10**, **11**, **13** and **6** for 24 h. Compounds were used at concentrations that gave maximal α-glucosidase I inhibition by FOS analysis (Table 1). Proteins from cell lysate were separated by SDS–PAGE and probed for BVDV E2 protein (Fig. 4). Treatment with 100 μM **11** caused an increase in apparent

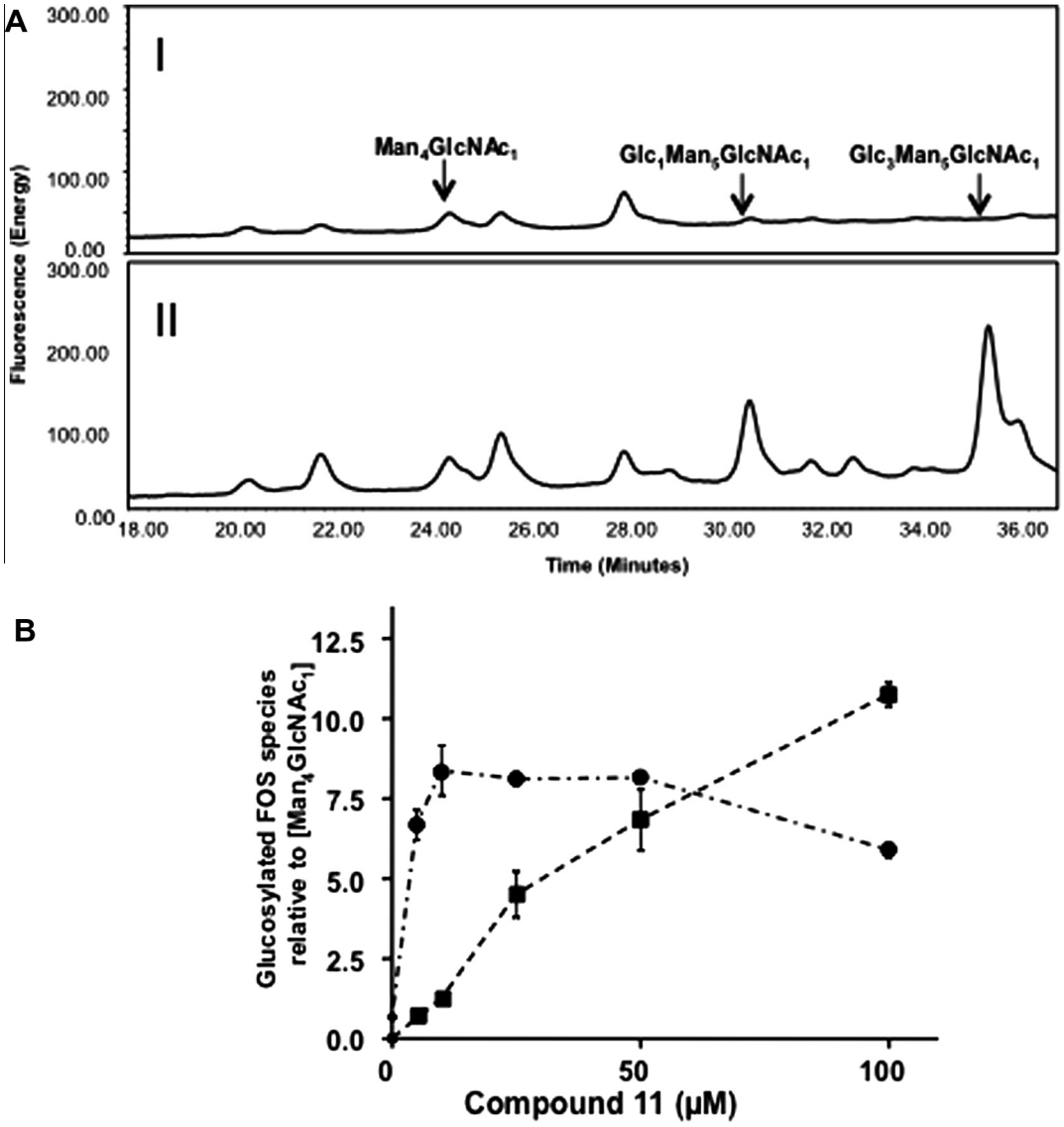

Figure 2. FOS analysis of adamantane–DNJ conjugates in MDBK cell. (A) Representative NP-HPLC profile of 2-AA labelled FOS analysis. (I) untreated MDBK cells and (II) 100 μM **11** administered for 24 h. Marked on the chromatograms are the $Man_4GlcNAc_1$ (which is constant in amount over all concentrations of inhibitor used in this study) and the mono- and tri-glucosylated $Man_5GlcNAc_1$ species which increase following α-glucosidase II and I inhibition respectively. (B) FOS dose response graph showing increases in mono- and tri-glucosylated $Man_5GlcNAc_1$ species relative to $Man_4GlcNAc_1$ following treatment with **11** up to 100 μM for 24 h. Circles, $Glc_1Man_5GlcNAc_1$; squares, $Glc_3Man_5GlcNAc_1$ oligosaccharides. Mean values are displayed, error bars show standard deviation.

molecular weight for all E2 species, due to increased glucosylation, whilst all other compounds showed little or no bandshift. For E1E2 heterodimer, the main band detected, there are six potential N-linked glycosylation sites.[17] A change in glycan structure from deglucosylated to triglucosylated could therefore increase the molecular weight of the heterodimer by up to 3.2 kDa (180.14 g/mol × 3 glucose residues × 6 glycosylation sites), which is in agreement with the bandshift observed.

4. Discussion

DNJ and its derivatives have shown antiviral activity against the flavivirus BVDV,[4] as well as a number of other viruses including hepatitis B virus,[18] and hepatitis C virus pseudoparticles.[19] DNJ-based iminosugars reversibly inhibit ER α-glucosidases I and II by competing with glucose substrates for their active site, thereby perturbing the folding of viral glycoproteins in the N-glycosylation pathway and impeding viral biogenesis by hindering their assembly.[20]

Disruption of the folding of envelope glycoproteins E1 and E2, essential for virus entry,[21] by ER α-glucosidase inhibition can induce misassembly of glycoprotein pre-budding complexes.[19]

The novel DNJ derivatives discussed here have been shown to inhibit ER α-glucosidases and to possess anti-viral activity against BVDV, with a distinct correlation observed between the increasing length of the alkyl chain linker between the DNJ head group and the triazole ring and their anti-viral efficacy. Compounds **7** and **8** demonstrate low levels of α-glucosidase II inhibition and little inhibition of α-glucosidase I even at the highest concentrations tested. Compounds **9** and **10**, which both possess a 4-carbon alkyl linker, show similar levels of inhibition of both enzymes, suggesting that the introduction of an ether bond in **10** between the triazole and adamantyl group has no effect on glucosidase inhibition. Longer alkyl chain compounds **11**, **12** and **13** efficiently inhibited α-glucosidase II at low concentrations (5–10 μM) and α-glucosidase I at high concentrations (25–100 μM). Compound **11** was able to attain the greatest level of α-glucosidase I inhibition, at similar concentrations to more hydrophobic compounds **12** and **13** that

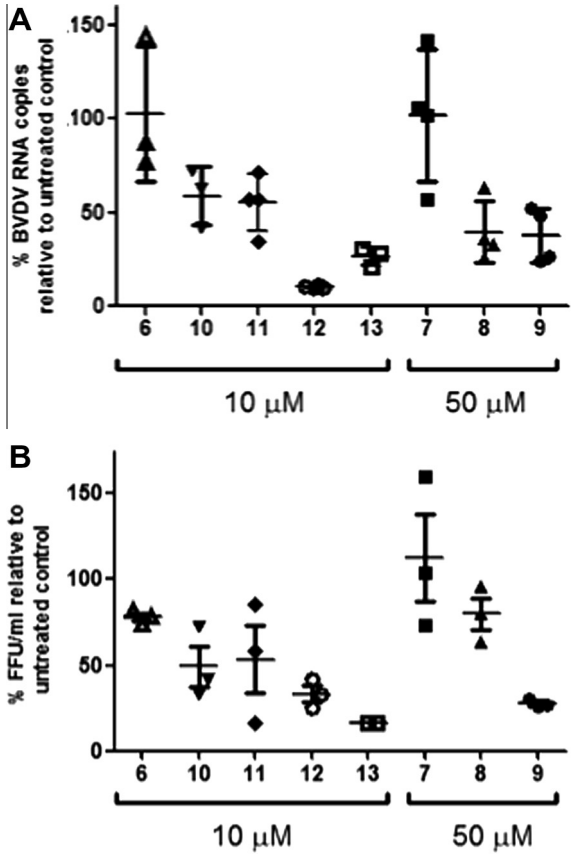

Figure 3. Antiviral results. (A) Quantification of secreted viral RNA levels. MDBK cells were infected with BVDV at an MOI of 1 (or mock-infected) and 10 μM **6**, **10**, **11**, **12** or **13**, or 50 μM **7**, **8** or **9** administered for 24 h. Cell culture supernatant was harvested and viral RNA purified and subjected to RT-PCR analysis, using primers against BVDV NS2 gene. (B) Fluorescence focus assay of BVDV-infected MDBK cells. MDBK cells were infected and administered with drug as described in Figure 3(A). Cell culture supernatant was harvested and fivefold serial dilutions were used to infect naive MDBK cells. After 24 h incubation, cells were fixed and probed with monoclonal antibody against BVDV NS2/3, followed by anti-mouse FITC-conjugated secondary antibody. Fluorescent focus units were counted and reduction in infection calculated relative to untreated control. The data were obtained from three experiments with means and standard deviations shown.

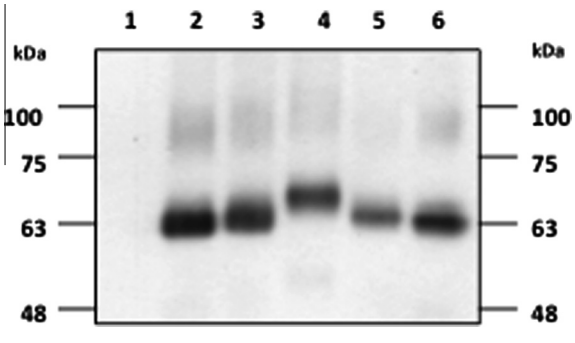

Figure 4. Western blot analysis of BVDV E2 protein. Western blot analysis of BVDV-infected MDBK cells. MDBK cells were mock-infected (Lane 1) or infected with BVDV at an MOI of 1 (Lanes 2–6) and treated with compounds for 24 h. Lane 2: Untreated control; 3: 100 μM **10**; 4: 100 μM **11**; 5: 10 μM **13**; 6: 100 μM **6**. After treatment, cells were lysed and proteins separated by SDS-10% PAGE, transferred to Immobilon-P PVDF membrane and probed with MAb214 against BVDV E2 protein. The main band observed, at 63 kDa in the untreated sample, is BVDV E1E2 heterodimer.

were used without affecting cell proliferation limiting their ability. The 6-carbon linker compound **11** could be administered to cells at higher concentrations and proved to be even more effective at inhibiting α-glucosidase I. In comparison to NAP-DNJ, an imino sugar which also contains a six carbon linker and is known to potently inhibit both α-glucosidases,[22] **11** achieves a comparable level of α-glucosidase I inhibition (Lee et al., manuscript in preparation). Increasing alkyl chain length in N-alkylated DNJ compounds has previously been shown to increase cellular uptake,[23] and an increase in the alkyl chain length linker between DNJ and phenyl or cyclohexyl groups increases ER α-glucosidase inhibition.[15] Here, increasing the alkyl chain length of the linker between DNJ and triazole group similarly increases α-glucosidase inhibition.

DNJ-based imino sugars have previously been shown to demonstrate antiviral activity against BVDV.[4] The longer alkyl chain *N*-nonyl-DNJ has shown tenfold greater potency than *N*-butyl-DNJ,[16] with branching and cyclization of side chains able to increase potency further.[24] Compound **7**, with a single carbon linker between DNJ and triazole, showed no anti-viral activity at the concentrations tested. As the length of the alkyl linker is increased, the amount of viral RNA in culture medium decreases, with 10 μM **12** reducing viral titre approximately tenfold. Compound **13** reduced viral titre less than **12**, suggesting an upper limit to alkyl linker length may have been reached. Subsequent infection of naive MDBK cells with virus secreted from cells administered with compound followed a similar pattern to α-glucosidase inhibition and viral secretion levels, although despite showing higher viral titre levels than **12**, less infection was observed following treatment with **13**. These results suggest that the antiviral effects of these compounds are largely a result of reduced viral biogenesis or secretion, rather than as a result of reduced infectivity, although an additional reduction is observed with **13**. In contrast, treatment with Adamantyl-DGJ **6**, a galactose analogue of Adamantyl–DNJ **10** that does not inhibit α-glucosidases, failed to reduce viral titre but partially reduced infectivity. Long-alkyl-chain DGJ derivatives have previously been shown to exert their antiviral effect solely via the production of viral particles with reduced infectivity,[16] which has been proposed to be through interaction with p7 ion channel.[25]

Direct effect on BVDV glycoprotein E2 is observed with Western blot analysis. Treatment with **11**, shown by FOS analysis to be the most potent α-glucosidase I inhibitor, resulted in increased glucosylation of intracellular E2 protein. These results taken together lead to the following proposal for the antiviral effects observed with compounds **7**–**13**. With the shorter alkyl chain compounds, antiviral activity is a result of ER α-glucosidase inhibition, which prevents efficient and successful processing of viral glycoproteins, resulting in a reduction in the formation of prebudding complexes and a subsequent reduction in viral formation and release. Increased hydrophobicity of longer alkyl linker derivatives facilitates their uptake and results in a prolonged period of retention in the intracellular environment where they can exert inhibition of α-glucosidases in the ER,[15] resulting in greater antiviral activity. Separately, as alkyl linker length increases, an antiviral effect unrelated to α-glucosidase inhibition begins to appear, producing non- or less infectious virions. Interactions between more hydrophobic adamantyl-conjugates and p7[25] may explain the reduction in infectivity. However, the improved ER-α-glucosidase inhibitory activity that appears to correlate with an effective reduction in viral titre and infectivity of these compounds, will allow further evaluation of their therapeutic potential.

Acknowledgments

The authors thank Professor Raymond Dwek and the Glycobiology Institute for support. This work was supported by the ANR program 'Jeunes Chercheuses—Jeunes Chercheurs', Project Number ANR-05-JCJC-0199.

References and notes

1. Stutz, A. E. *Iminosugars as Glycosidase Inhibitors*; Wiley-VCH: Weinheim, 1999.
2. Butters, T. D.; Dwek, R. A.; Platt, F. M. *Chem. Rev.* **2000**, *100*, 4683.
3. Norez, C.; Noel, S.; Wilke, M.; Bijvelds, M.; Jorna, H.; Melin, P.; DeJonge, H.; Becq, F. *FEBS Lett.* **2006**, *580*, 2081.
4. Zitzmann, N.; Mehta, A. S.; Carrouee, S.; Butters, T. D.; Platt, F. M.; McCauley, J.; Blumberg, B. S.; Dwek, R. A.; Block, T. M. *Proc. Natl. Acad. Sci. U.S.A.* **1999**, *96*, 11878.
5. Chang, J.; Schul, W.; Yip, A.; Xu, X.; Guo, J. T.; Block, T. M. *Antiviral Res.* **2011**, *92*, 369.
6. Butters, T. D.; Wormald, M. R.; Dwek, R. A.; Platt, F. M.; Van Den Broek, L. A. G. M.; Fleet, G. W. J.; Krulle, T. M. *Tetrahedron: Asymmetry* **2000**, *11*, 113.
7. Compain, P.; Martin, O. R. *Iminosugars. From Synthesis to Therapeutic Applications*; John Wiley & Sons Ltd: Chichester, 2007.
8. Cox, T.; Lachmann, R.; Hollak, C.; Aerts, J.; van Weely, S.; Hrebicek, M.; Platt, F.; Butters, T.; Dwek, R.; Moyses, C.; Gow, I.; Elstein, D.; Zimran, A. *Lancet* **2000**, *355*, 1481.
9. Elstein, D.; Hollak, C.; Aerts, J. M.; van Weely, S.; Maas, M.; Cox, T. M.; Lachmann, R. H.; Hrebicek, M.; Platt, F. M.; Butters, T. D.; Dwek, R. A.; Zimran, A. *J. Inherit. Metab. Dis.* **2004**, *27*, 757.
10. Ardes-Guisot, N.; Alonzi, D. S.; Reinkensmeier, G.; Butters, T. D.; Norez, C.; Becq, F.; Shimada, Y.; Nakagawa, S.; Kato, A.; Bleriot, Y.; Sollogoub, M.; Vauzeilles, B. *Org. Biomol. Chem.* **2011**, *9*, 5373.
11. Greimel, P.; Spreitz, J.; Stutz, A. E.; Wrodnigg, T. M. *Curr. Top. Med. Chem.* **2003**, *3*, 513.
12. Norton, A.; Gu, B.; Block, T. M. Iminosugars. From Synthesis to Therapeutic Applications In Compain, P., Martin, O. R., Eds.; John Wiley & Sons Ltd: Chichester, 2007; p 209.
13. Alonzi, D. S.; Neville, D. C.; Lachmann, R. H.; Dwek, R. A.; Butters, T. D. *Biochem. J.* **2008**, *409*, 571.
14. Neville, D. C.; Coquard, V.; Priestman, D. A.; te Vruchte, D. J.; Sillence, D. J.; Dwek, R. A.; Platt, F. M.; Butters, T. D. *Anal. Biochem.* **2004**, *331*, 275.
15. Alonzi, D. S.; Dwek, R. A.; Butters, T. D. *Tetrahedron: Asymmetry* **2009**, *20*, 897.
16. Durantel, D.; Branza-Nichita, N.; Carrouee-Durantel, S.; Butters, T. D.; Dwek, R. A.; Zitzmann, N. *J. Virol.* **2001**, *75*, 8987.
17. Dubuisson, J.; Rice, C. M. *J. Virol.* **1996**, *70*, 778.
18. Block, T. M.; Lu, X.; Platt, F. M.; Foster, G. R.; Gerlich, W. H.; Blumberg, B. S.; Dwek, R. A. *Proc. Natl. Acad. Sci. U.S.A.* **1994**, *91*, 2235.
19. Chapel, C.; Garcia, C.; Bartosch, B.; Roingeard, P.; Zitzmann, N.; Cosset, F. L.; Dubuisson, J.; Dwek, R. A.; Trepo, C.; Zoulim, F.; Durantel, D. *J. Gen. Virol.* **2007**, *88*, 1133.
20. Parodi, A. J. *Biochem. J.* **2000**, *348*, 1.
21. Ronecker, S.; Zimmer, G.; Herrler, G.; Greiser-Wilke, I.; Grummer, B. *J. Gen. Virol.* **2008**, *89*, 2114.
22. Rawlings, A. J.; Lomas, H.; Pilling, A. W.; Lee, M. J.; Alonzi, D. S.; Rountree, J. S.; Jenkinson, S. F.; Fleet, G. W.; Dwek, R. A.; Jones, J. H.; Butters, T. D. *ChemBioChem* **2009**, *10*, 1101.
23. Mellor, H. R.; Platt, F. M.; Dwek, R. A.; Butters, T. D. *Biochem. J.* **2003**, *374*, 307.
24. Mehta, A.; Ouzounov, S.; Jordan, R.; Simsek, E.; Lu, X.; Moriarty, R. M.; Jacob, G.; Dwek, R. A.; Block, T. M. *Antiviral Chem. Chemother.* **2002**, *13*, 299.
25. Pavlovic, D.; Neville, D. C.; Argaud, O.; Blumberg, B.; Dwek, R. A.; Fischer, W. B.; Zitzmann, N. *Proc. Natl. Acad. Sci. U.S.A.* **2003**, *100*, 6104.